Velocity analysis using prestack depth migration: applying the linear theory

John T. Etgen

ABSTRACT

The linear theory I presented in the previous SEP report can be used to predict the effect a change in the interval-slowness model has on prestack depth-migrated constant-offset sections. The effects we can detect are changes in the curvature of the images of reflectors over offset and a pull-up or push-down of the reflectors along their normals. An example shows that the linear theory can predict the change in curvature over offset and pull-up or push-down of a reflector due to a local anomaly interval slowness above the reflector. A generalized inverse of the linear operator applied to measured changes in residual curvature can be used to estimate the slowness anomalies above the reflector. I plan to use the linear theory to drive an iterative nonlinear inversion that estimates interval slowness models to use for prestack depth migration.

INTRODUCTION

In SEP–59 (Etgen, 1988) I described a linear theory that relates changes of the interval-slowness model used for prestack depth migration to changes in a residual moveout correction that best stacks migrated constant-offset sections. This linear operator is similar to the one Toldi (1985) derived and used to estimate interval slowness above horizontal reflectors. Fowler (1988) extended Toldi's operator to use either prestack time migration or dip-moveout (DMO) corrected constant-velocity stacking as an imaging operator rather than simple constant-velocity stacking. The operator I describe, like Toldi's and Fowler's, is a form of reflection tomography.

Rather than use prestack time migration or normal moveout (NMO) to image the subsurface reflectors, I depth-migrate constant-offset sections of the data before stack. Because only prestack depth migration accounts for ray bending due to lateral velocity variation, using prestack depth migration rather than DMO or

prestack time migration should improve resolution of both the position of reflectors and the overburden velocity when geologic structure is complex and the overburden velocity varies strongly laterally. Moreover, since applying the linear operator involves a reflection tomography calculation; using prestack depth migration to position reflectors mitigates the problem of finding the spatial location of reflectors needed for the tomography calculation (Stork, 1988).

If the data were migrated with the correct interval velocity model, any residual "shift" correction applied over offset to the images of any reflector will degrade the stacked image of the reflector; simply stacking the images of the reflector over offset produces the best image. However, if the interval velocity model was in error, some residual moveout correction will enhance the coherency of the reflector images over offset and produce a better stack.

When using NMO or prestack time migration, moveout corrections are parameterized by stacking or migration velocity (or slowness). The stacking slowness, which can be measured directly, is some function of the interval-slowness model. Unfortunately, prestack depth migration depends directly on the interval-slowness model and has no intermediate parameter such as stacking velocity or prestack time-migration velocity that can be measured directly. It is difficult to find what effect a change in the velocity model has on the position and offset coherence of reflectors without remigrating the data. To get around this problem, a residual-moveout correction that is a function of a parameter resembling residual stacking slowness can be applied after constant-offset prestack depth migration. Using this residual moveout, a pseudo-velocity space that resembles velocity stacks can be formed. The variation of the stack semblance with residual slowness can be analyzed for variations in the overburden interval slowness in a manner like Toldi analyzed variations in NMO-stacking slowness.

The linear operator described in my previous report provides a relation between the intermediate parameter which I will interchangeably call residual curvature or residual slowness and the interval-slowness model needed for prestack depth migration. I hope to correct errors in the overlying interval slowness model by inverting the relation between the measured spatially variable residual slowness at each reflector point and the overlying interval-slowness model.

Examples of applying the linear operator demonstrate how the linear operator estimates the effects of slowness perturbations on migrated and residual-moveout corrected constant-offset sections. Further examples describe inverting the linear operator to estimate perturbations to the interval-slowness model given measured changes in the best-fitting residual moveout along a reflector.

VISUALIZING THE LINEAR OPERATOR

The detailed derivation of the linear operator can be found in SEP–59 (Etgen, 1988); I will not present it here for brevity's sake. The linear operator between

changes in the interval slowness used for prestack depth migration and the residual slowness that best stacks the image can be written as:

$$\begin{pmatrix} \Delta\gamma \\ \Delta\sigma_o \end{pmatrix} = \begin{pmatrix} G_\gamma \\ G_{\sigma_o} \end{pmatrix} \Delta w \quad . \tag{1}$$

The change in the interval-slowness model has two effects on the image of a reflector a change in the residual slowness that best stacks the reflector and a pull-up or push-down of the reflector along the zero-offset ray; these are denoted by $\Delta\gamma$ and $\Delta\sigma_o$ respectively.

Figure 1 shows the effect a point anomaly in interval slowness has on a continuous sequence of horizontal reflectors. The "cone" of the operator shows which points in the image are affected by the anomaly. Only those points on the reflectors that have specular rays that pass through the anomaly are affected. The plot shows the two parts of the linear operator, the top plot predicts changes in the curvature of the best residual moveout curve; the bottom plot predicts the motion of the position of the reflector. These changes are a function position since the offset which "sees" the anomaly at a given reflector point depends on the position of the reflector point beneath the anomaly. Outside the cone of the operator, reflector points on a flat reflector are not affected by the anomaly because no specularly reflected ray from those points passes through the anomaly and falls within the recording cable.

Figure 2 shows the effect of a point anomaly in interval slowness on a continuous sequence dipping reflectors. As above, both parts of the operator are shown; but now the second part of the operator predicts motion normal to the reflectors rather than simply up and down. The "cone" of the operator shows those positions on the dipping reflectors that are affected by the slowness anomaly. The operator cone is tilted with respect to the operator for the horizontal reflector because the rays that specularly illuminate the reflectors are tilted along the normal to the reflectors.

On the top plots of Figures 1 and 2, the areas lighter than the grey background represent reflectors whose residual slowness is increased by the presence of the anomaly. The areas darker than the grey background represent reflector points whose residual slowness is decreased by the presence of the anomaly. On the bottom plots of Figures 1 and 2, the areas lighter than the grey background are reflector points that are pushed down due to the presence of the anomaly. Areas darker than the background are reflector points pulled up by the presence of the anomaly.

PREDICTING RESIDUAL SLOWNESS ANOMALIES

Using the linear operator for forward modeling predicts the curvature and zero-offset intercept change of the best-fitting residual-moveout curve due to a small change in the interval-slowness model.

As an example, I created a synthetic survey using finite-differences for a model with a single reflector with horizontal and dipping segments. The model contained

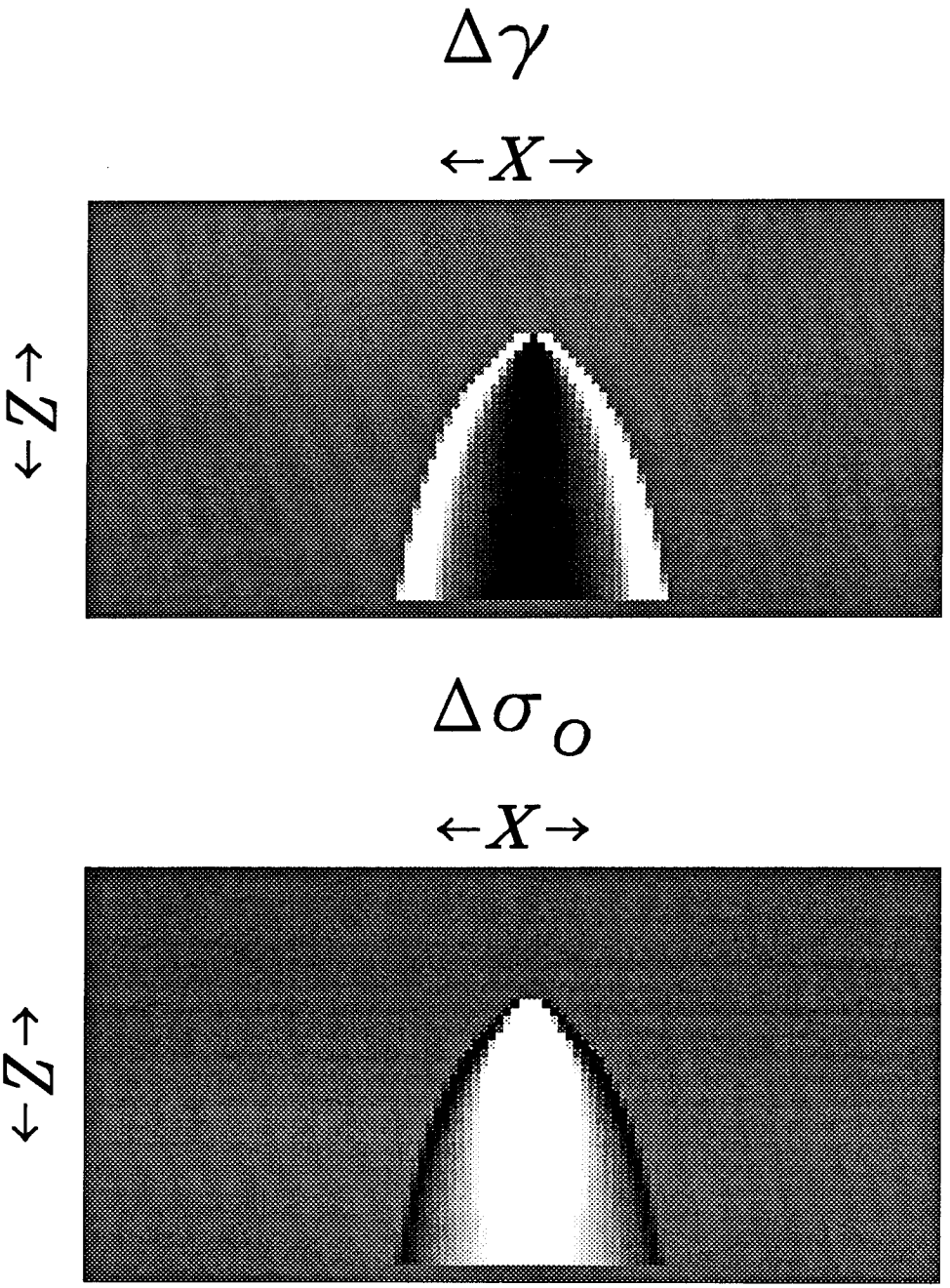

FIG. 1. Response of the linear operator to a point anomaly in interval slowness predicting changes in residual slowness (top) and pull-up or push-down of the reflector image (bottom) for a sequence of horizontal reflectors. Light areas represent increases in residual slowness at a reflector point (top) or push-down of the image of the reflector (bottom). Dark areas represent decreases in residual slowness (top) or pull-up of the reflector image (bottom).

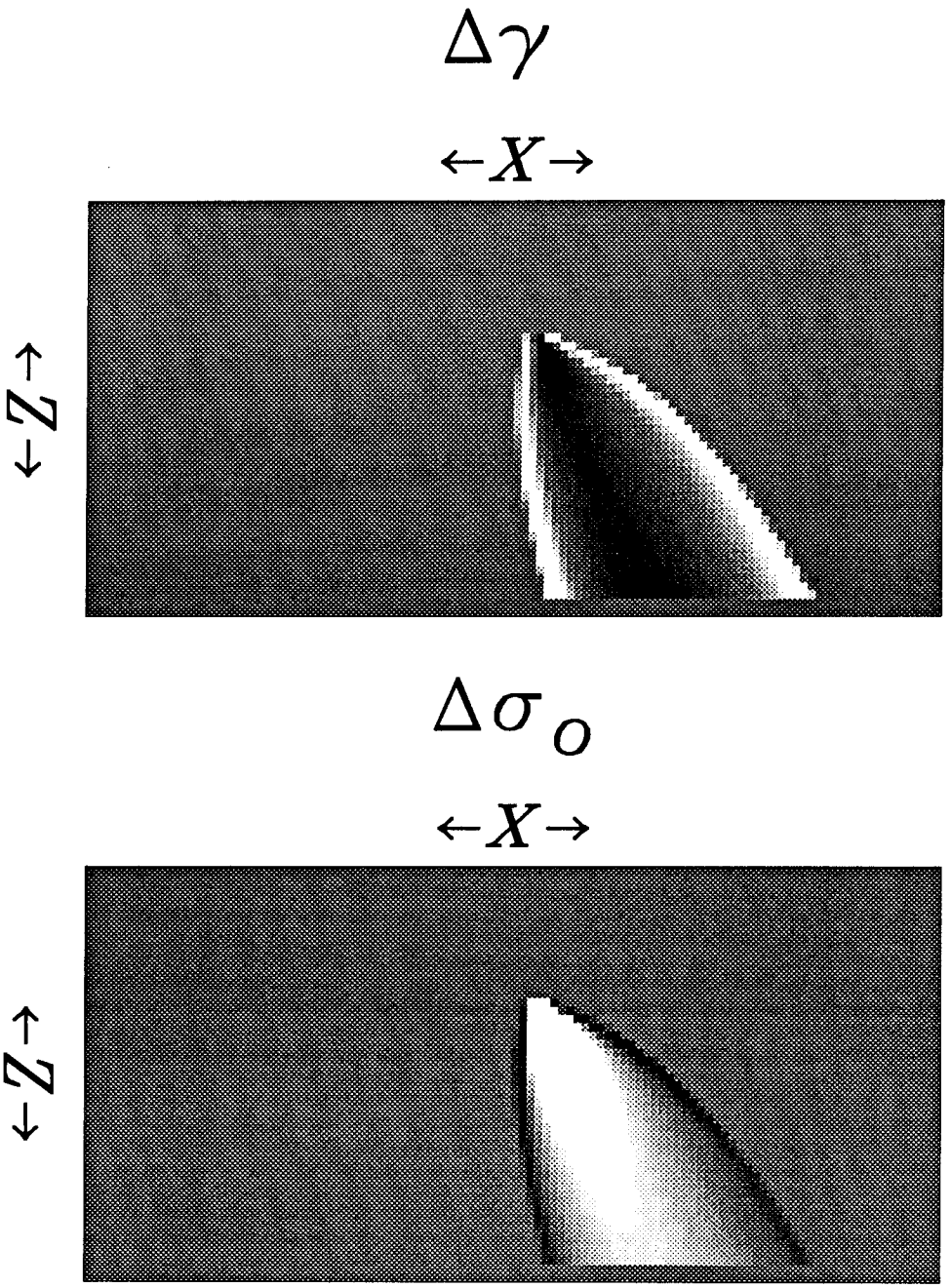

FIG. 2. Response of the linear operator to a point anomaly in interval slowness predicting changes in residual slowness (top) and pull-up or push-down of the reflector image (bottom) for a sequence of dipping reflectors. Light areas represent increases in residual slowness at a reflector point (top) or push-down of the image of the reflector along its normal (bottom). Dark areas represent decreases in residual slowness (top) or pull-up of the reflector image (bottom).

two velocity anomalies, one above the horizontal segment of the reflector (low velocity), and one above the dipping segment of the reflector (high velocity). Figure 3 shows schematically the positions and shapes of the anomalies and the reflector position. I migrated the multi-fold data before stack with a constant velocity equal

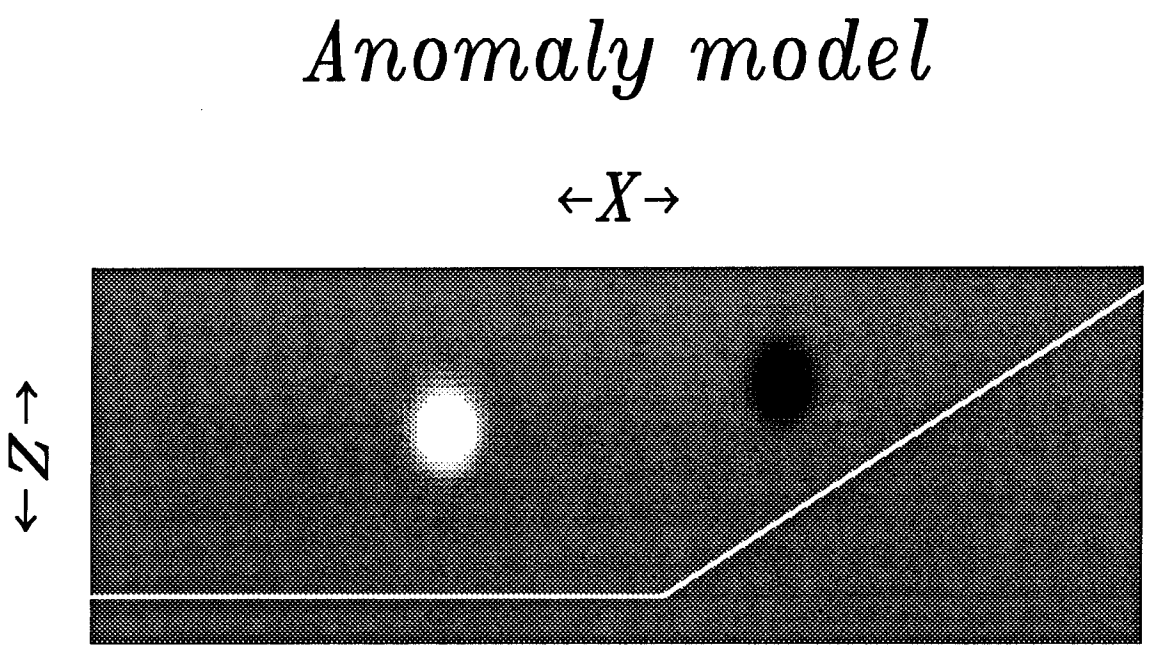

FIG. 3. Model used to make synthetic dataset. The left anomaly is a positive slowness anomaly with maximum amplitude 12% of the background slowness. The right anomaly is a negative slowness anomaly 9% of the background slowness. The white line is the reflector position.

to the velocity of the model away from the anomalies. The migrated zero-offset and far-offset sections are shown in Figure 4. The effect of the anomaly above the horizontal reflector can be clearly seen as a push-down of the reflector at the midpoints that have rays that go through the anomaly. The effect of the anomaly above the dipping reflector is a pull-up but is not as pronounced because the magnitude of the perturbation in slowness above the dipping was smaller than above the horizontal reflector.

Figure 5 shows two common reflection point gathers; the left gather had its inner-offsets pushed down relative to the outer-offsets; the right gather had its outer-offsets pushed down relative to its inner-offsets. Residual moveout and stack was applied to the migrated constant-offset sections for a range of residual slowness. Figure 6 shows stack-semblance versus residual slowness for the two common-reflection-point gathers of Figure 5. The reflector whose inner-offsets were perturbed by the anomaly stacks best at a residual slowness below one, corresponding to upward curvature over offset. The reflection point that had outer-offsets perturbed by the anomaly stacks best at a residual slowness greater than one corresponding to downward curvature over offset.

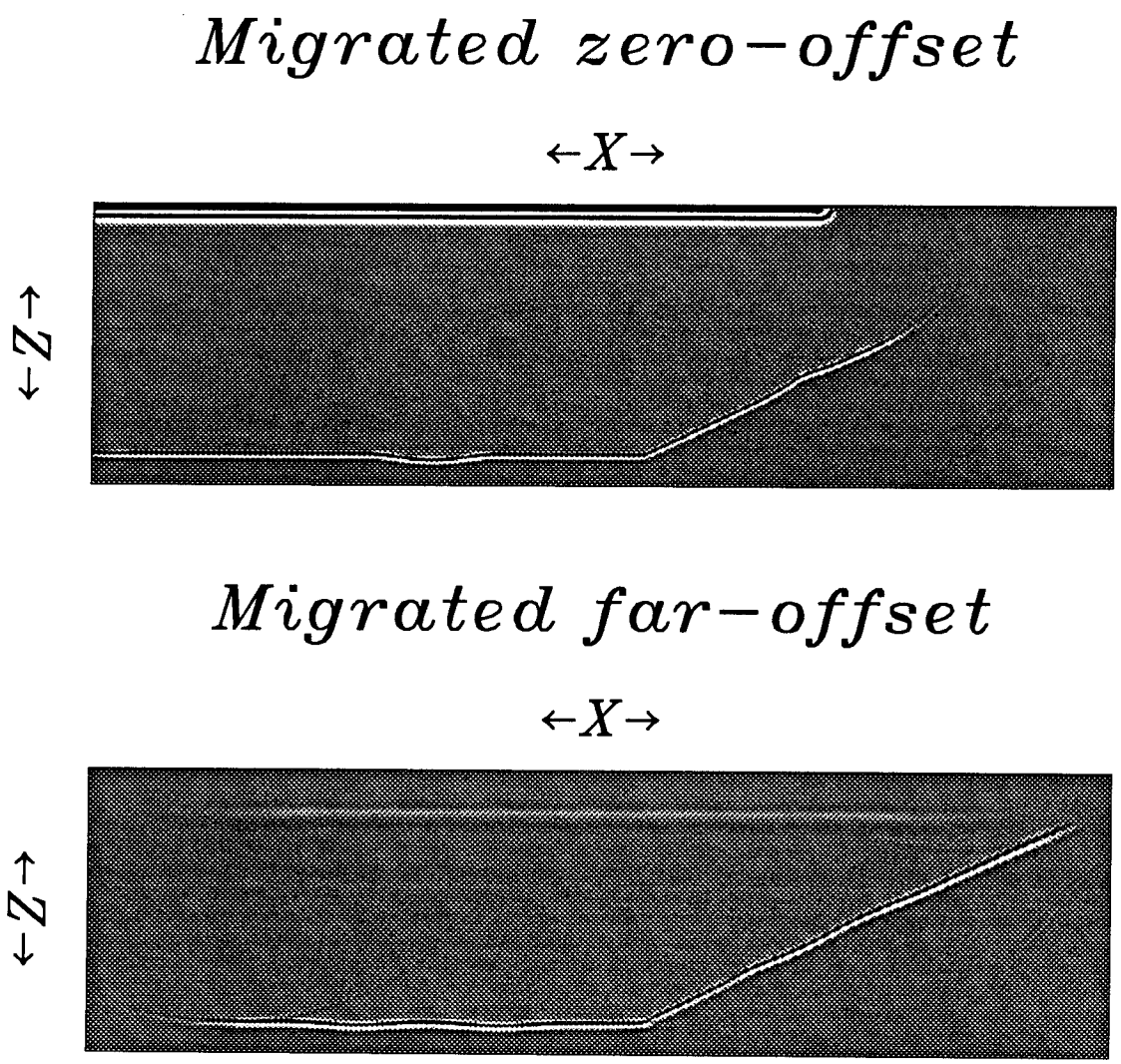

FIG. 4. Migrated zero-offset section (top) and migrated far-offset section. Migration ignored the slowness anomalies, so their effects can be seen on the images as pull-ups (dipping reflector) or push-downs (flat reflector).

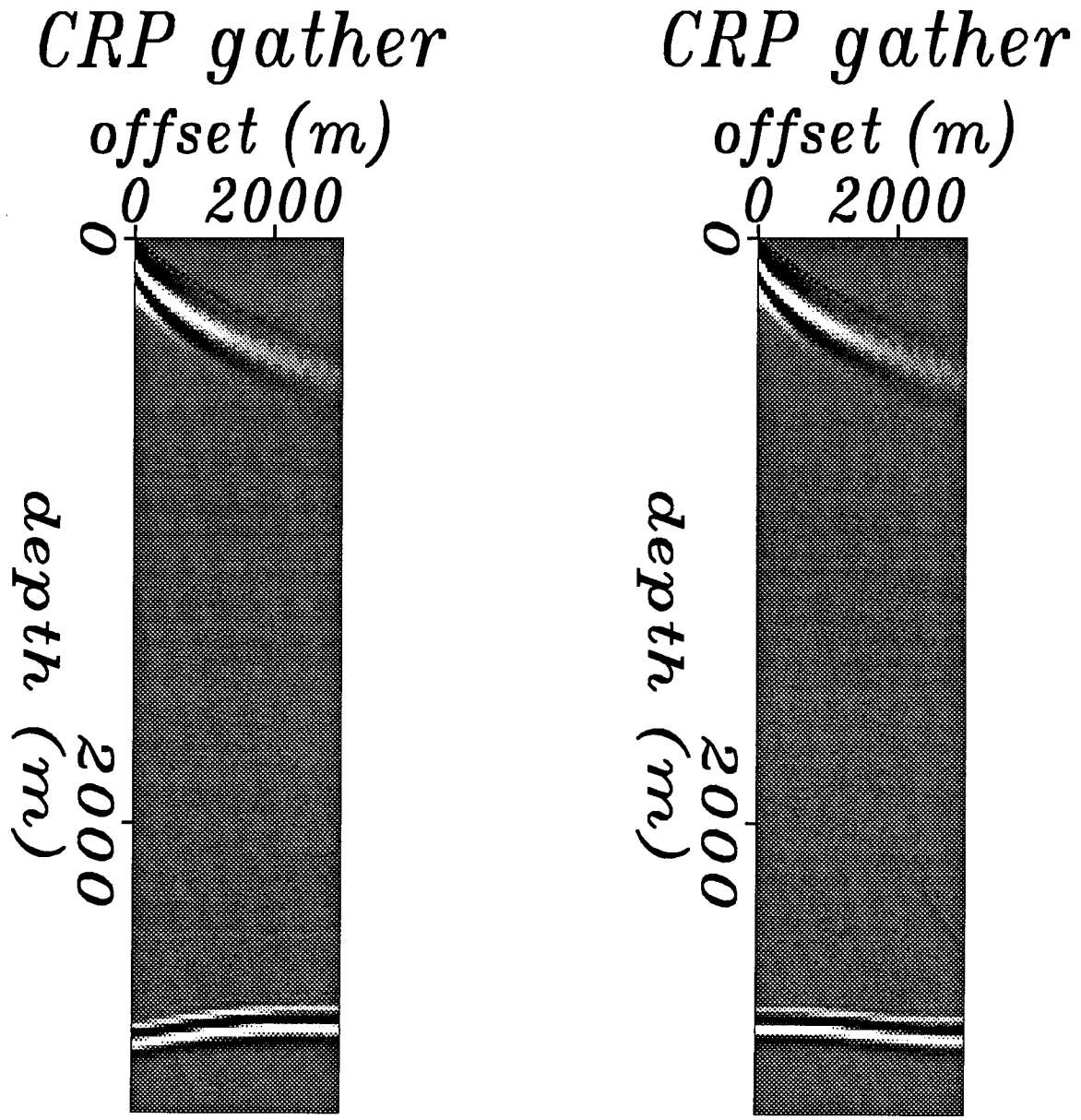

FIG. 5. Common-reflector-point gathers at a reflection point whose inner offsets were perturbed by the anomaly above the flat reflector (left) and at a reflection point whose outer offsets were perturbed by the anomaly above the flat reflector (right).

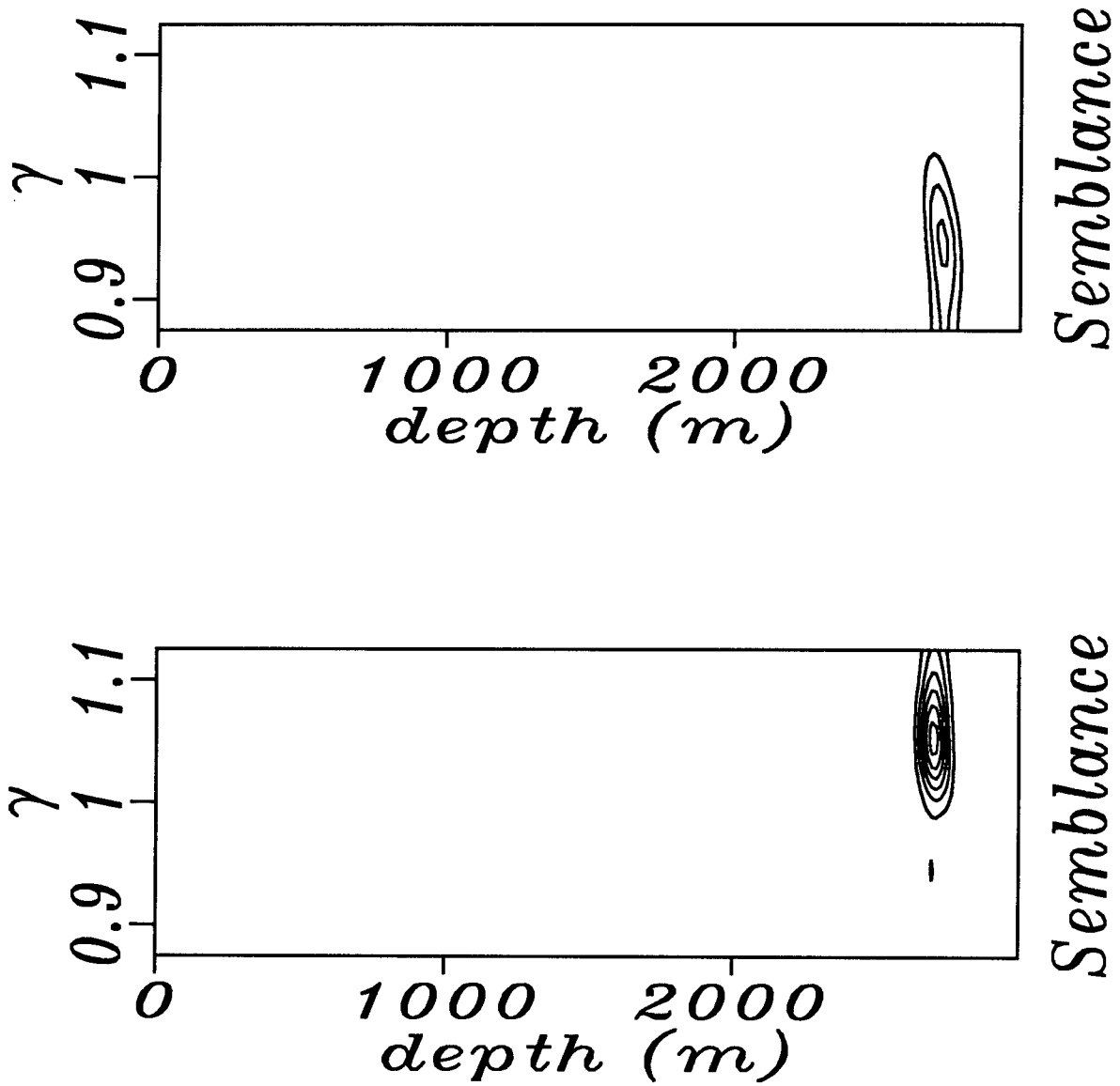

FIG. 6. Contoured stack semblance versus residual curvature γ. Residual slowness increases ($\gamma > 1$) for the reflector point whose outer offsets were perturbed (bottom). Residual slowness decreases ($\gamma < 1$) for the reflector point whose inner offsets were perturbed (top).

Figure 7 shows the result of picking the maximum of the stacking semblance versus reflector point, depth, and residual slowness γ to give the reflector location and residual slowness at each reflection point. The linear operator can be used to predict the effects of the slowness anomalies that were measured. Figure 8 shows the predicted effect of the slowness anomalies of the model on a sequence of flat reflectors for the left anomaly and a sequence of dipping reflectors for the right anomaly. Of course, the synthetic data only has one reflector; but I display the resulting changes in residual slowness and position of the reflectors for several hypothetical reflectors to illustrate the behavior of the operators. Figure 9 is the result of extracting along the true reflector position the residual slowness and change in reflector position predicted by the linear operator and comparing this prediction with the measured values. Measured values are dashed, predicted values are solid lines. The predicted values using the linear operator closely match the observed values.

ESTIMATING INTERVAL SLOWNESS ANONALIES

The inverse to the linear operator can be used to estimate perturbations to an interval-slowness model using the measured residual slowness as function of position on underlying reflectors. In general, we only measure the residual slowness of a reflector, and do not know its true spatial position, so we can only invert the top equation in equation (1).

$$\Delta w = G_\gamma^{-g} \Delta\gamma \ ; \tag{2}$$

where the $-g$ superscript means generalized inverse since the operator G_γ is usually not square. The most practical generalized inverse will be the damped least squares inverse

$$\Delta w = (G_\gamma^T G_\gamma + \lambda I)^{-1} G_\gamma^T \Delta\gamma \ . \tag{3}$$

If G_γ is singular or nearly so, then we cannot hope to estimate the slowness anomaly perfectly. It is easy to see that any slowness perturbation that moves the reflector but does not change the residual slowness at any point along the reflector (i.e. $G_{\sigma_o} \neq 0$, $G_\gamma = 0$) cannot be estimated by equation (2). This is a form of the "velocity–reflector depth ambiguity" of velocity estimation based on curvature over offset. If the structure is known, or can be constrained, then a joint inversion of residual slowness and pull-up push-down is possible.

$$\Delta w = \begin{pmatrix} G_\gamma \\ G_{\sigma_o} \end{pmatrix}^{-g} \begin{pmatrix} \Delta\gamma \\ \Delta\sigma_o \end{pmatrix} \ . \tag{4}$$

The linear operator is formally a filtered traveltime tomography operator; inverting the linear operator resembles solving a traveltime tomography problem. The linear operator reduces all the information contained in traveltime versus offset at each image point to the residual slowness and zero-offset of the best fitting residual moveout curve. So, in addition to solving the traveltime tomography problem, the inversion removes the effects of the residual moveout and stack filter. Since the

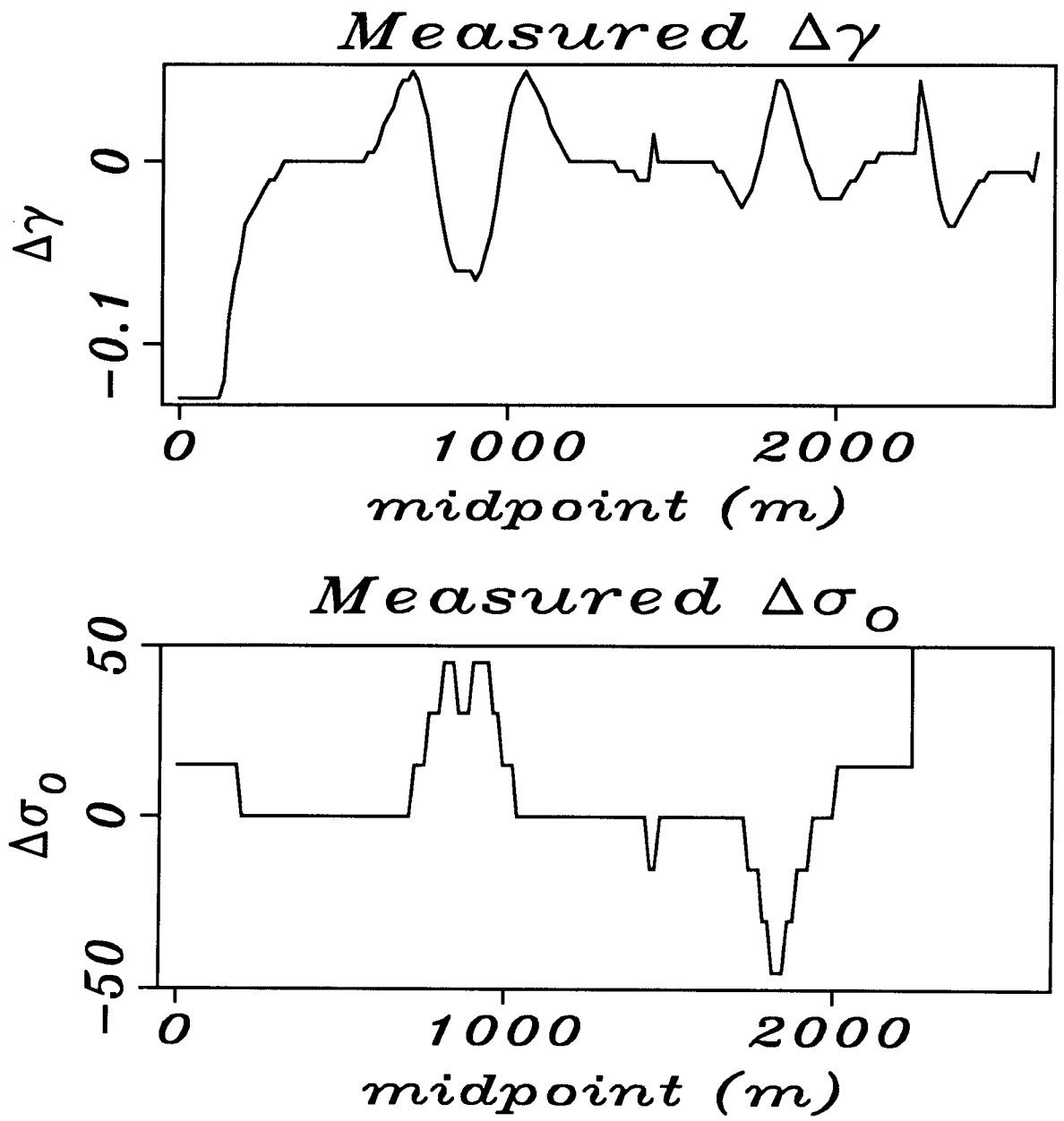

FIG. 7. Picked value of the change in residual slowness $\Delta\gamma$ (top) and change in the position of the reflector $\Delta\sigma_o$ (bottom) for each point along the reflector. Below 500 m and above 2 500 m the curves are only noise. The reflector is only imaged between 500 m and 2 500 m.

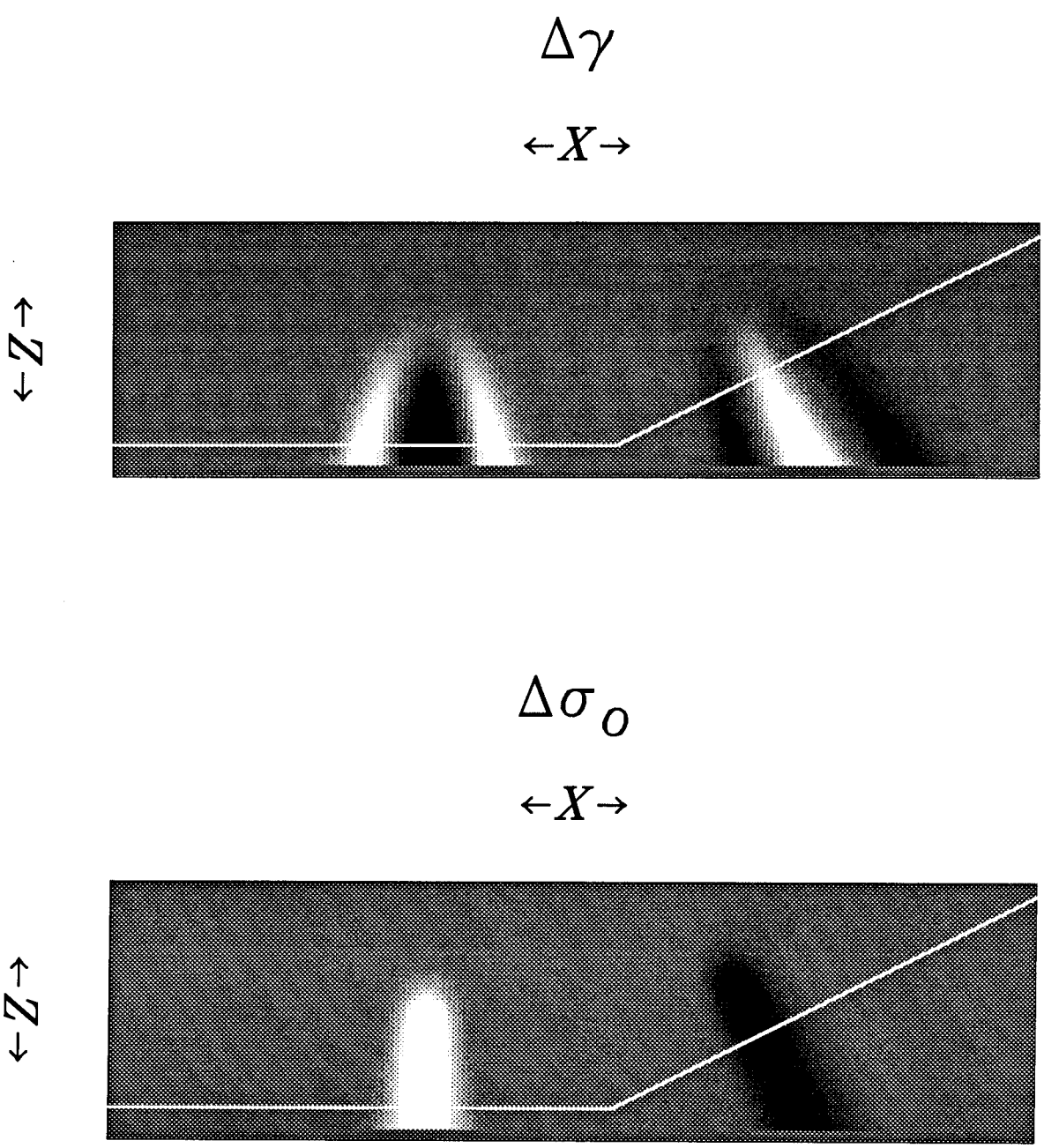

FIG. 8. Predicted changes in residual slowness (top) and reflector position (bottom) for a sequence of flat reflectors near the left anomaly and a sequence of dipping reflectors near the right anomaly. White areas are increases in γ and σ_o and dark areas are decreases in γ and σ_o. Grey areas represent no change.

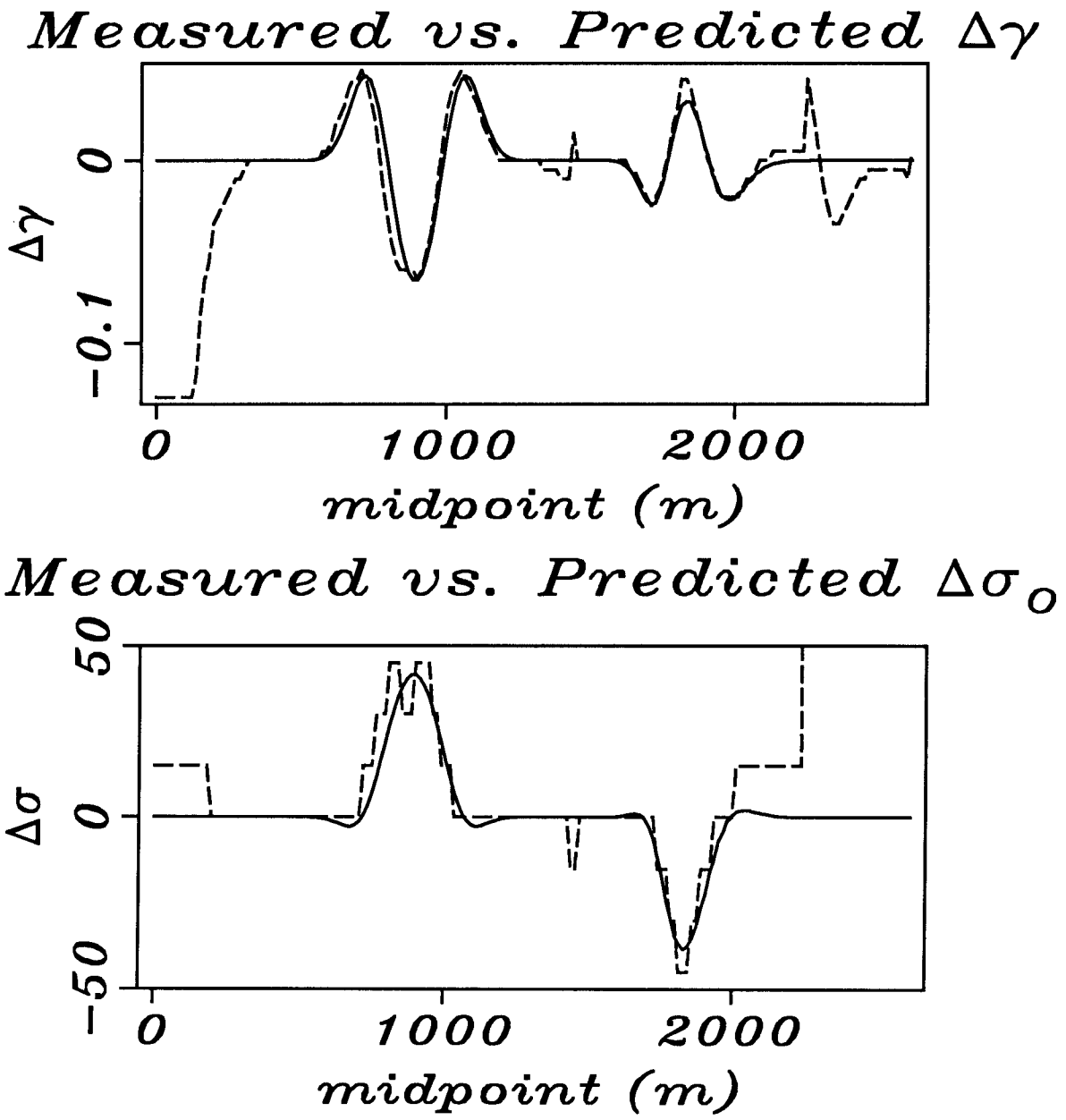

FIG. 9. Comparison of the predicted change (solid lines) in residual slowness (top) and the change in reflector position (bottom) to the measured change (dashed lines) in the residual slowness and reflector position.

filtering done by residual moveout and stack can add no new information (Fowler, 1988), the upper bound on the resolution of estimated slowness anomalies obtained by inverting equation (2) is the resolution obtained by standard traveltime tomography. In fact, since the effects of the residual moveout and stack filter cannot be completely removed (the above velocity–reflector depth ambiguity), the resolution of inverting equation (2) is less than standard traveltime tomography.

However, when applying picked traveltime tomography to real data, there is often difficulty identifying reflections and picking their traveltimes. Migrating the data before stack and applying residual moveout and stacking increases the signal to noise ratio of the reflection events. It should be much easier to pick maxima of stack semblance rather than traveltimes in raw data. Moreover, using the linear operator allows picking to be abandoned entirely. Rather than minimizing the distance between our predicted residual slowness and the picked residual slowness, maximize the total semblance obtained by summing through the semblance panels at the residual slowness predicted for each midpoint and all depths. The maximum value of the sum will be obtained when the predicted residual slowness overlies the maxima of the stack semblance for all reflectors.

Using the measured residual slowness of the previous section, I solved equation (3) for an estimate of the slowness anomalies. The slowness model has many more degrees of freedom than the number of residual slowness picks when only one or a few reflectors are used so a least squares inverse of the linear operator is required. I did not include the change in the reflector depth as data for the inversion. To solve the underdetermined least squares system I used Paige and Saunders' LSQR algorithm (1982).

Figure 10 shows the resulting estimate of the slowness anomalies. There are two main artifacts of interest. The first artifact, common to all tomography methods is the streaks due to limited ray-angle coverage. The second effect is the large sidelobes on the estimated anomalies. The sidelobes are present because the effects of the moveout and stack filter are not completely removed at the anomaly locations. When more reflectors are present, the anomaly is "seen" with many different effective cable lengths (Toldi, 1985), and the effects of the moveout and stack filter can be more completely removed. Figure 11 shows a purely synthetic inversion obtained by forward modeling using the linear operator for two reflector levels and then estimating the slowness anomalies using equation (3). The estimated anomalies now have much smaller artifacts because the anomalies were seen by two different effective cable lengths.

SUMMARY

The linear operator I presented in SEP–59 can be used for modeling the effect changes in the interval-slowness model used for prestack depth migration have on migrated constant-offset sections. Inverting the linear operator is a equivalent to

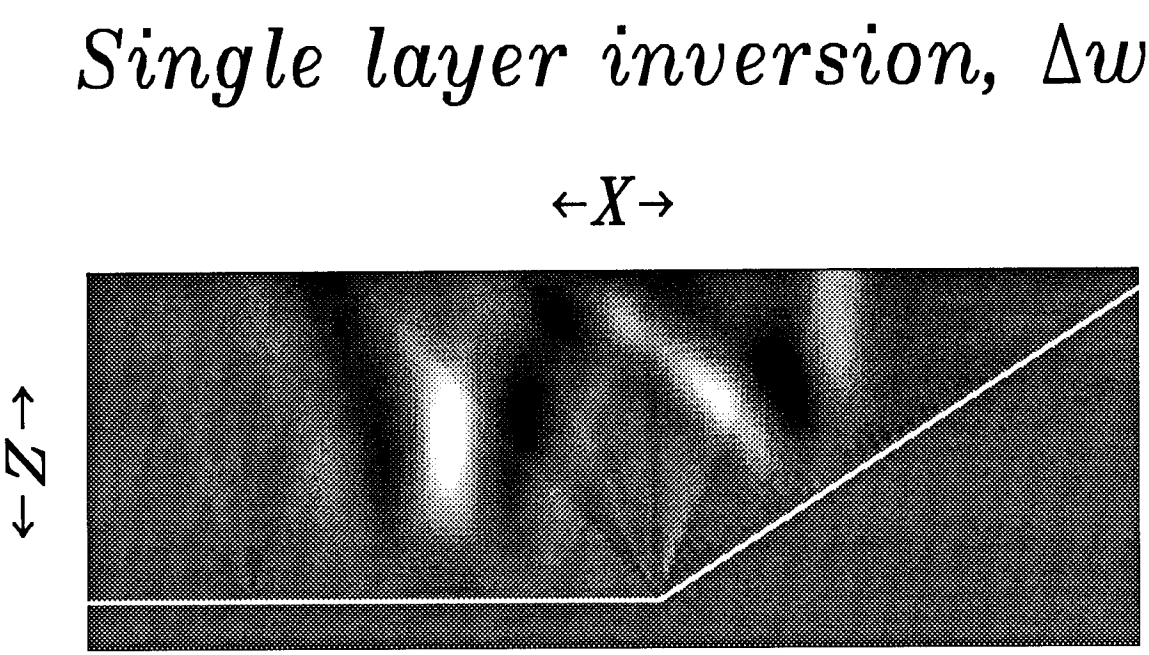

FIG. 10. Single reflector inversion using the picked residual slowness from Figure 7. Both anomalies are found, but sidelobes appear on the inversion results. The white line is the reflector position.

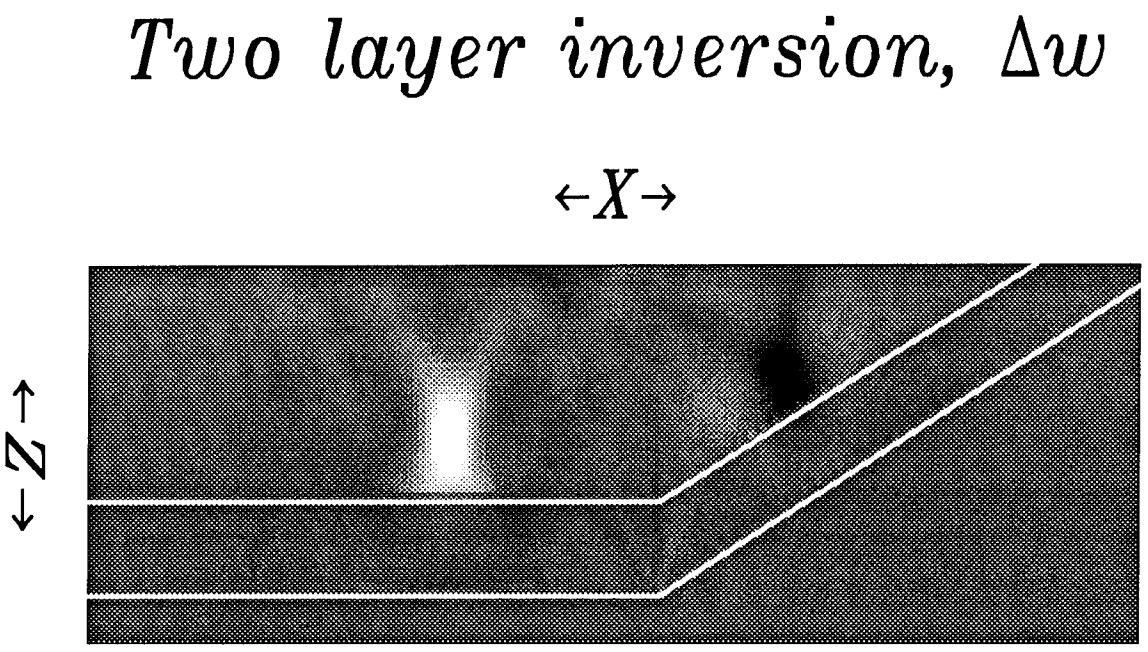

FIG. 11. Two reflector inversion using synthetic data forward modeled by the linear operator. When there are more layers to measure residual slowness along, the sidelobes disappear; the inversion can better localize the slowness anomalies. The white lines are the hypothetical reflectors.

solving a filtered traveltime tomography problem and can estimate interval-slowness anomalies from measured changes in residual slowness.

ACKNOWLEDGMENTS

I thank Biondo Biondi and Jos Van Trier for interesting discussions on velocity analysis.

REFERENCES

Al Yahya, K., 1987, Velocity analysis by profile migration: Ph.D. Thesis, Stanford University; also SEP–**53**, 11-30.

Etgen, J., 1988, Velocity analysis by prestack depth migration: linear theory revised: SEP–**59**, 121-140.

Fowler, P., 1988, Seismic velocity estimation using prestack migration: Ph.D. Thesis, Stanford University; also SEP–**58**, 1–185.

Toldi, J., 1985, Velocity analysis without picking: Ph.D. Thesis, Stanford University; also SEP–**43**, 1-103.

Paige, C. C., and Saunders, M. A., 1982, LSQR: an algorithm for sparse linear equations and sparse least squares: ACM Transactions on Mathematical Software, **8**, 43–71.

Stork, C., 1988, Ray trace tomographic velocity analysis of surface seismic reflection data: Ph.D. thesis, California Institute of Technology.